Journal of Organometallic Chemistry 735 (2013) 58–64

Contents lists available at SciVerse ScienceDirect

Journal of Organometallic Chemistry

journal homepage: www.elsevier.com/locate/jorganchem

Tetrahedral silicon-based luminescent molecules: Synthesis and comparison of thermal and photophysical properties by various effect factors

Dengxu Wang [a,b], Linlin Wang [b], Lei Xue [b], Debo Zhou [b], Shengyu Feng [b,*], Xian Zhao [a,*]

[a] State Key Laboratory of Crystal Materials, Shandong University, Jinan 250100, PR China
[b] Key Laboratory of Special Functional Aggregated Materials, Ministry of Education, School of Chemistry and Chemical Engineering, Shandong University, Jinan 250100, PR China

ARTICLE INFO

Article history:
Received 29 January 2013
Received in revised form
2 March 2013
Accepted 7 March 2013

Keywords:
Photoluminescence
Silane
Imidazole
Pyrazole
Benzimidazole

ABSTRACT

A series of luminescent molecules were presented employing the tetrahedral structural motif of the silicon atom, which further connected different N-containing heterocycle functional groups in their periphery using phenyl rings as the bridges. These compounds included three kinds of N-heterocycle functional silanes: imidazole derivatives (**1a**–**h**), pyrazole derivatives (**2a**–**e**) and benzimidazole derivatives (**3a**–**b**), and their structures were fully characterized by FT-IR, ^{1}H NMR, ^{13}C NMR and HRMS. The TGA results indicate that they all exhibit high thermal stabilities. The photophysical properties demonstrate that they are fluorescent in the violet-blue region and could be potentially applied as blue emitters for organic light-emitting diodes (OLEDs). The effect factors of sort, disposition and number of substituent groups and N-containing heterocycle functional groups on their thermal and photophysical properties were investigated. Molecular calculations were also performed to support the experimental results. Moreover, the computational results reveal that these compounds all exhibit relatively large HOMO–LUMO band gaps with the range from 4.82 eV (**2d**) to 5.19 eV (**1a** and **2c**), making them become promising candidates as host materials for emitters and hole/electron blocking materials in OLEDs display.

1. Introduction

In recent years, organic luminescent materials have attracted intense interest in the chemistry and material science because of their potential applications in sensor technologies as well as organic light-emitting diodes (OLEDs) [1–16]. Compared with other small organic molecules and polymers, luminescent materials based on tetrahedral organosilicon compounds have many advantages: (i) easy accessibility and well-defined structures; (ii) high color purity as evidenced by narrow emissions in solution and solid films [17,18]; (iii) conjugation blocking for a wide band gap [19,20] and (iv) high thermal stability and good film-forming properties with a relatively high glass transition temperature (T_g) for non-aggregating amorphous morphology [21,22]. Moreover, organosilicon compounds can be extensively applied as blue emitting materials [17,18,23], carrier transport materials [24] and phosphorescent host materials [25–28] for OLEDs. Therefore, a large amount of silicon-based luminescent materials have been designed, synthesized and utilized to fabricate highly efficient blue, green, red and white OLEDs [17–33].

Usually organosilicon compounds applied for OLEDs were synthesized by combining luminescent functional groups (commonly aromatic condensed rings or heterocycle groups) with silicon atom. Compared to the compounds containing condensed rings, those containing heterocycle groups are easier to dissolve in common solvents and thus more easily processed. Furthermore, they are more easily modified. For instance, after interacting with metal complexes, their photophysical properties can be tuned and their applications can be extended [34–36]. Moreover, it is demonstrated that they could be used as intriguing building blocks to construct functional metal-organic frameworks (MOFs) with interesting molecular topologies and potentially applied in many fields such as gas adsorption, ion exchange, molecular separation, etc [37–41].

Obviously the structures of these compounds have a significant effect on the thermal stability, luminescent properties and thus on the performance of electroluminescent devices. As previous reports, there are many effect factors on the luminescent properties, including the sort, disposition and number of functional groups and substituent groups [42,43]. However, systematic study of

* Corresponding authors. Tel.: +86 531 8836 4866; fax: +86 531 8856 4464.
E-mail addresses: fsy@sdu.edu.cn (S. Feng), zhaoxian@sdu.edu.cn (X. Zhao).

0022-328X/$ – see front matter © 2013 Elsevier B.V. All rights reserved.
http://dx.doi.org/10.1016/j.jorganchem.2013.03.010

silicon-based luminescent materials and the effect factors has not been attempted.

Previously we have synthesized several functional silanes containing N-heterocycle groups, which locate in the phenyl-bridged *para*-disposition. Their photophysical properties revealed that they could be potentially applied as blue emitters or hole-blocking materials for OLEDs [44,45]. Meanwhile, using these compounds as tetrahedral ligands, MOFs with 1D, 2D and 3D structures and specific properties were also constructed [46,47]. Based on our research, herein we prepared a series of novel silanes with N-heterocycle as functional groups, including imidazole, pyrazole and benzimidazole in the phenyl-bridged *para*-disposition as well as compounds with N-heterocycle groups in the phenyl-bridged *meta*-disposition. Then a comprehensive investigation encompassing thermal stability, photophysical property as well as the theoretical modeling on these compounds was presented in this article. Moreover, effect factors including the sort, disposition and number of substituent groups and functional groups on thermal stability and luminescent properties were also discussed.

2. Results and discussions

2.1. Synthesis

In our previous report, a series of imidazole functionalized silanes with imidazole locating in the phenyl-bridged *para*-disposition, including $Me_2Si(p\text{-}C_6H_4\text{-imdazol-1-yl})_2$ (**1a**), $MeSi(p\text{-}C_6H_4\text{-imdazol-1-yl})_3$ (**1b**), $Ph_2Si(p\text{-}C_6H_4\text{-imdazol-1-yl})_2$ (**1c**), $PhSi(p\text{-}C_6H_4\text{-imdazol-1-yl})_3$ (**1d**) and $(p\text{-}C_6H_4Br)Si(p\text{-}C_6H_4\text{-imdazol-1-yl})_3$ (**1e**) were synthesized *via* mono-lithiation, Si–C coupling reaction and copper-mediated Ullmann condensation reaction [44]. Under the same condition, we firstly synthesized a series of bromophenylsilanes, including (4-bromophenyl)silanes (**4a**–**f**) and (3-bromophenyl)silanes (**5a**–**c**). To investigate the position effect of functional groups, three novel imidazole silanes with imidazole locating in the phenyl-bridged *meta*-disposition, including $Me_3Si(m\text{-}C_6H_4\text{-imdazol-1-yl})$ (**1f**), $Me_2Si(m\text{-}C_6H_4\text{-imdazol-1-yl})_2$ (**1g**) and $MeSi(m\text{-}C_6H_4\text{-imdazol-1-yl})_3$ (**1h**) were achieved based on **5a**–**c** and imidazole (Scheme 1). To study the effect of different functional groups, silanes with pyrazole and benzimidazole as functional groups were also successfully obtained (Scheme 1). The synthetic condition was similar to that of **1a**–**h**. Pyrazole derivatives include $Me_2Si(p\text{-}C_6H_4\text{-pyrazol-1-yl})_2$ (**2a**), $Ph_2Si(p\text{-}C_6H_4\text{-pyrazol-1-yl})_2$ (**2b**), $MeSi(p\text{-}C_6H_4\text{-pyrazol-1-yl})_3$ (**2c**), $PhSi(p\text{-}C_6H_4\text{-pyrazol-1-yl})_3$ (**2d**) and $Me_2Si(m\text{-}C_6H_4\text{-pyrazol-1-yl})_2$ (**2e**) and benzimidazole derivatives include $Me_2Si(p\text{-}C_6H_4\text{-benimidazol-1-yl})_2$ (**3a**), $Ph_2Si(p\text{-}C_6H_4\text{-benimidazol-1-yl})_2$ (**3b**), $Me_2Si(m\text{-}C_6H_4\text{-benimidazol-1-yl})_2$ (**3c**).

Apparently, the functional groups in these compounds connect to the silicon atom with the phenyl ring as the bridge, further forming a tetrahedral structure. Moreover, these compounds can be divided into two kinds: (i) the functional groups locate in the *para*-disposition, including **1a**–**e**, **2a**–**d**, **3a** and **3b**; (ii) the functional groups locate in the *meta*-disposition, including **1f**–**h**, **2e** and **3c**. The successful synthesis of these compounds proves that the position effect is limited under this method. The results also demonstrate that this method is an effective means to synthesize N-heterocycle silanes from bromophenylsilanes and N–H containing N-heterocycle compounds. Furthermore, these compounds were fully characterized by FT-IR, ^{1}H NMR, ^{13}C NMR and HRMS.

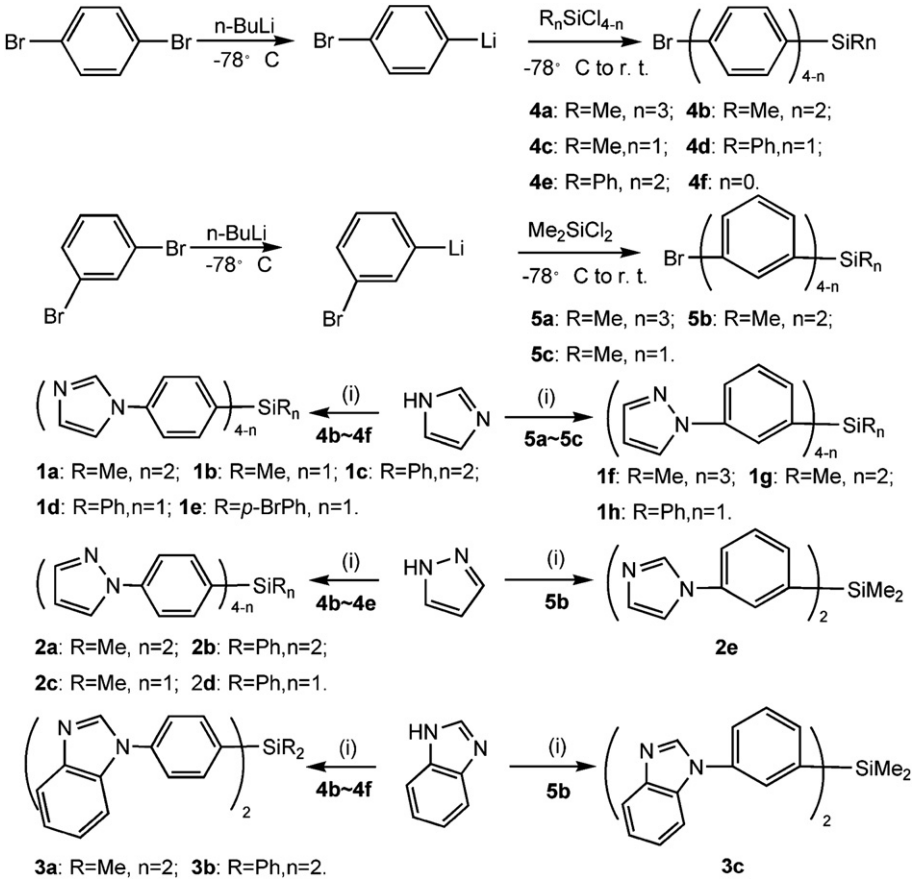

Scheme 1. The synthetic routes of N-heterocycle functional silanes, **1a**–**h**, **2a**–**e** and **3a**–**c**. (i) $CuSO_4$, K_2CO_3, 180 °C, 24 h.

2.2. Thermal property

The thermal properties of these compounds were determined by thermogravimetric analysis (TGA) and differential scanning calorimetry (DSC) measurements (Fig. S1–S2). The results indicate that they exhibit high thermal decomposition temperatures (T_d corresponding to 5% weight loss) in the range of 230–367 °C. Unfortunately, most of their T_g were not obviously observed except **1h** and **3a** showing at 70 °C and 93 °C, which are substantially higher than those of tetraarylsilane compounds (26–53 °C) [19,48], indicating that the introduction of N-heterocycle groups improves their morphological stability. With the same substituent groups and disposition linkage, benzimidazole derivatives exhibit higher thermal stability than imidazole and pyrazole derivatives. In addition, compounds with phenyl substituent and a *para*-disposition linkage show higher thermal ability than those with methyl substituent and a *meta*-disposition connection.

2.3. Photophysical properties and molecular calculations

Fig. 1 shows the electronic absorption of imidazole derivatives (**1f**–**h**), pyrazole derivatives (**2a**–**e**) and benzimidazole derivatives (**3a**–**c**) in CH_2Cl_2 solution and the resulting spectral data are summarized in Table 1. Compounds **1f**–**h** exhibit two similar intense absorption bands with λ_{max} at ~230 nm and ~250 nm, which are short blue-shifted compared with **1a**–**e** [44]. **2a**–**d** also show two absorption peaks with λ_{max} at ~230 nm and ~270 nm and the absorption band of **2e** with λ_{max} at 227 nm and 259 nm are observed with short blue shift compared with **2a**–**d**. Different from imidazole and pyrazole derivatives, benzimidazole derivatives (**3a**–**c**) display three intense absorption bands with λ_{max} at ~230 nm, ~260 nm and ~280 nm, while **3c** also show short blue-shifted absorption compared with **3a** and **3b**. Obviously, these absorption peaks of all these compounds can be assigned to the π–π^* transitions involving the phenyl and N-heterocycle groups.

All the compounds emit a violet to blue color in solution and the solid state when irradiated by UV light (Figs. 2 and 3). In CH_2Cl_2 solution, **1f**–**h** show similar emission peaks with λ_{max} at ~310 nm, which is consistent with **1a**–**e** in our previous report [44]. Compounds **2a**–**e** and **3a**–**c** also display analogic fluorescence spectra with λ_{max} at ~310 nm and ~325 nm, respectively. For pyrazole derivatives, **2c** and **2d** with three pyrazole groups exhibit higher luminescent intensity than **2a** and **2b** with two pyrazole groups and this phenomenon is also observed in imidazole derivatives, indicating that introducing more functional groups is beneficial to enhance the luminescent intensity. However, among all these silanes, phenyl-substituted compounds (such as **2b**, **2d**) don't display higher luminescent intensity than methyl-substituted ones (such as **2a**, **2c**), although higher electronic density exists in phenyl group than methyl group, indicating that the contributions of the substituted groups on their optical properties are limited. Benzimidazole derivatives emit at a somewhat longer wavelength than imidazole and pyrazole derivatives, which can be attributed to the higher π-conjugated system with higher electron density in benzimidazole than that in imidazole and pyrazole. Moreover, the emission energy in solution shows a slightly red shift (~5 nm) from compounds with a *para*-disposition linkage (such as **1a**, **2a**, **3a**) to those with a *meta*-disposition connection (such as **1g**, **2e**, **3c**).

In the solid state, the emission spectra of all the compounds are considerably red shifted, compared to that in solution, which is possibly caused by the various intermolecular interactions, such as π–π stacking interactions as proved in **1a** by our previous report [44]. For **1g** and **1h**, a broad emission was observed mainly from violet to blue region with λ_{max} at 408 and 410 nm. Compared to the imidazole derivatives, **2a**–**d** exhibit a narrower emission in the voile–blue region and the λ_{max} of emission ranges from 329 nm (**2c**) to 356 nm (**2b**). For **3a**–**c**, a broad emission in the violet-blue region was also observed, which is similar to imidazole and pyrazole derivatives. Interestingly, **3c** appears to emit a larger red-shift than the other two analogs, indicating that different intermolecular interactions in **3c** may exist. Unfortunately, the emission quantum efficiencies of these compounds are low and vary between 0.051 (**1e**) and 0.12 (**2a**). As our previous report, the low quantum efficiencies may be attributed to two reasons: (i) low π-conjugated degree of aromatic rings in these compounds and (ii) limited $d\pi$–$p\pi$ conjugation effect of the silicon core [44]. However, the introduction of silicon atom to these compounds can improve color purity due to the narrow emission, which makes these compounds become promising candidates for blue emitters in OLEDs displays.

To achieve a deeper insight into the structure–property of the compounds at the molecular level, molecular orbital calculations have been performed at the B3LYP/6–31G(d) level using the Gaussian 03 suite of programs [49]. The HOMO and LUMO contour plots, HOMO, LOMO energies and energy gap of these compounds are shown in Fig. 4 and Fig. S3. For **1g** and **1h**, the HOMO orbitals are predominantly located on the imidazolyl moiety, while LUMOs involve contributions from entire molecules. The results are consistent with other imidazole derivatives, **1a**–**e** [44], which explain why the photophysical properties of **1g** and **1h** are similar to those of **1a**–**e**. For pyrazole derivatives, **2a**–**e**, the HOMO and LUMO orbitals are similar, with dominating contributions from entire molecules, which is different from **1a**–**h**. For benzimidazole derivatives, **3a**–**c**, the HOMO and LUMO orbitals also involve contributions from entire molecules. It is noted that different substituent groups don't have an obvious effect on the electronic orbital, which agrees with experimental results as mentioned above. In addition, the calculated band gaps for benzimidazole derivatives

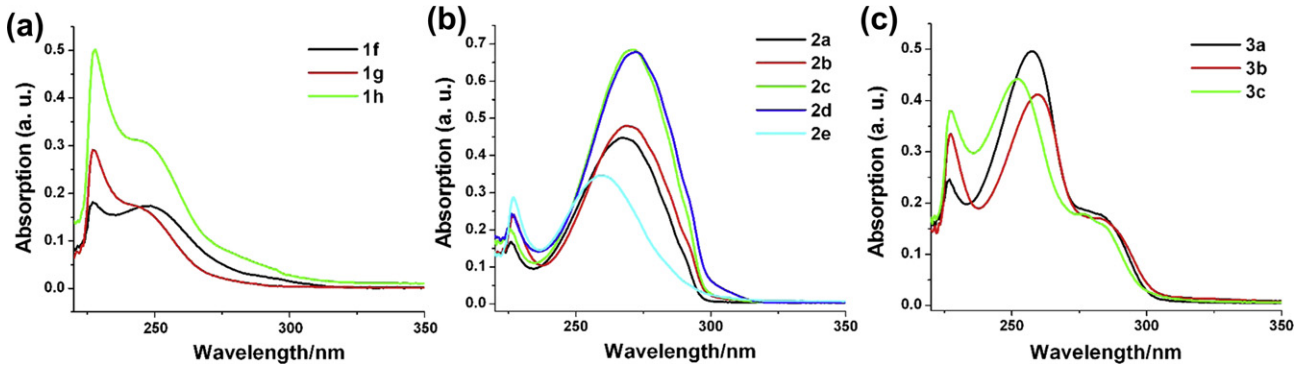

Fig. 1. UV–vis absorption of **1**–**h** (a), **2a**–**e** (b) and **3a**–**c** (c) in CH_2Cl_2 solution.

Table 1
Physical data of compounds **1a**–**h**, **2a**–**e** and **3a**–**c**.

Compound	λ_{abs} (nm)[a]	$\lambda_{em,\ max}$ (nm)[a,b]	Quantum yield	Conditions (298 K)	HOMO/LUMO/band gap (eV)	T_d/T_g (°C)[c]
1a	252, 227	309	0.094	CH_2Cl_2	−6.18/−0.99/5.19	
		395		solid state		245/–
1b	254, 227	315	0.062	CH_2Cl_2	−6.28/−1.13/5.15	
		398		solid state		318/–
1c	254, 228	308	0.093	CH_2Cl_2	−6.19/−1.10/5.09	
		356		solid state		338/–
1d	255, 228	312	0.073	CH_2Cl_2	−6.28/−1.28/5.00	
		388		solid state		345/–
1e	256, 228	313	0.051	CH_2Cl_2	−6.34/−1.39/4.95	
		399		solid state		270/–
1f	248, 227	304	–	CH_2Cl_2	–/–/–	
		–		solid state		–/–
1g	246, 227	306	0.078	CH_2Cl_2	−6.17/−0.95/5.12	
		408		solid state		285/70
1h	247, 228	309	0.061	CH_2Cl_2	−6.25/−1.12/5.13	
		410		solid state		265/–
2a	268, 227	309	0.15	CH_2Cl_2	−5.90/−0.90/5.00	
		342		solid state		262/–
2b	270, 227	309	0.084	CH_2Cl_2	−5.93/−0.92/5.01	
		356		solid state		318/–
2c	271, 226	310	0.066	CH_2Cl_2	−6.20/−1.01/5.19	
		329		solid state		356/–
2d	272, 226	311	0.070	CH_2Cl_2	−5.93/−1.01/4.82	
		346		solid state		230/–
2e	259,227	311	0.062	CH_2Cl_2	−5.87/−0.79/5.08	
		–		solid state		215/–
3a	283, 257, 227	325	0.058	CH_2Cl_2	−5.99/−0.97/5.02	
		339		solid state		340/93
3b	284, 259, 227	325	0.070	CH_2Cl_2	−5.99/−1.06/4.93	
		371		solid state		367/–
3c	277, 253, 227	324	0.059	CH_2Cl_2	−5.95/−0.95/5.00	
		344		solid state		286/–

[a] Sample concentrations for compounds **1a**–**h**, **2a**–**e** and **3a**–**c** were ca. 1×10^{-6} M in CH_2Cl_2.
[b] The excitation wavelengths were 250 nm and 280 nm in solution and in the solid state.
[c] T_d is defined as the temperature at which a 5% weight loss is recorded by the TGA analysis.

are smaller than most of imidazole and pyrazole derivatives, which is consistent with the experimentally observed trend and the fact that the benzimidazole derivatives have a relatively longer emission wavelength. On the basis of the MO calculation results, the observed electronic and luminescence for these compounds can be assigned to $\pi-\pi^*$ transitions. The results also prove that the tetrahedral silicon core interrupts the conjugation of the functional groups segments and thus does not have significant effects on the electronic properties. However, the introduction of silicon into materials may endow them large band gaps. As expected, these compounds all own a relatively large band gaps with the range from 4.82 eV (**2d**) to 5.19 eV (**1a** and **2c**), making them potentially used as hosting materials for emitters and hole/electron blocking layer in OLEDs display.

3. Conclusion

Tetrahedral silicon-based luminescent compounds with three series of N-heterocycle functional groups, including imidazole, pyrazole and benzimidazole, and different substituent groups have been designed, synthesized and characterized. TGA measurements reveal that all the compounds have high thermal stability. Compounds **1h** and **3a** also show high T_g as determined by DSC, indicating that they also possess high morphological stability. The photophysical properties and molecular calculations demonstrate that these functional silanes could be potentially applied as blue emitters, host materials as well as hole/electron blocking materials for OLEDs. Furthermore, effect factors on their luminescent properties and thermal stability were also investigated. The results

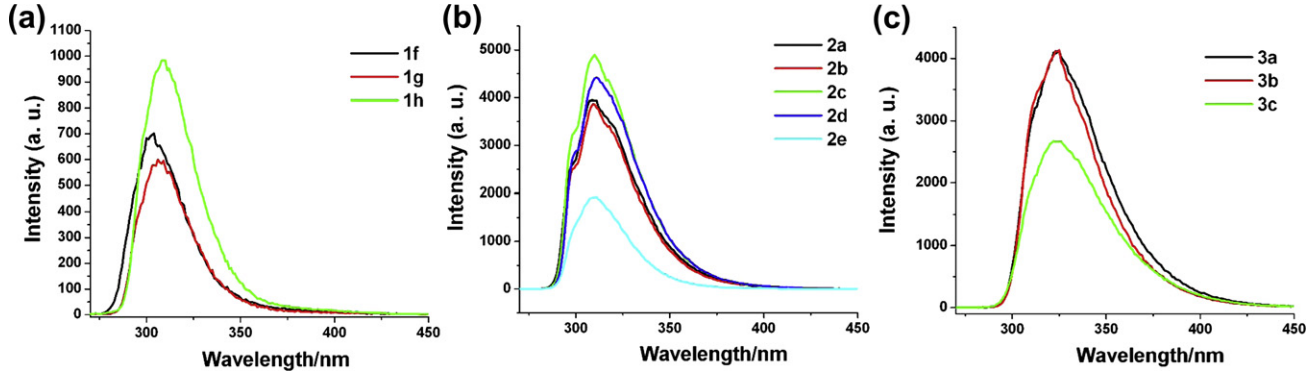

Fig. 2. Emission spectra of **1f**–**h** (a), **2a**–**e** (b) and **3a**–**c** (c) in CH_2Cl_2 solution.

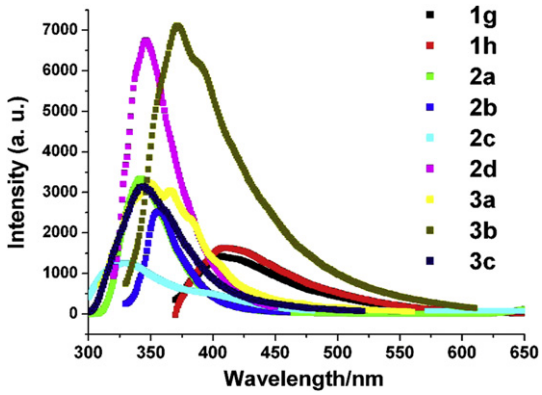

Fig. 3. Emission spectra of **1g**–**h**, **2a**–**d** and **3a**–**c** in the solid state.

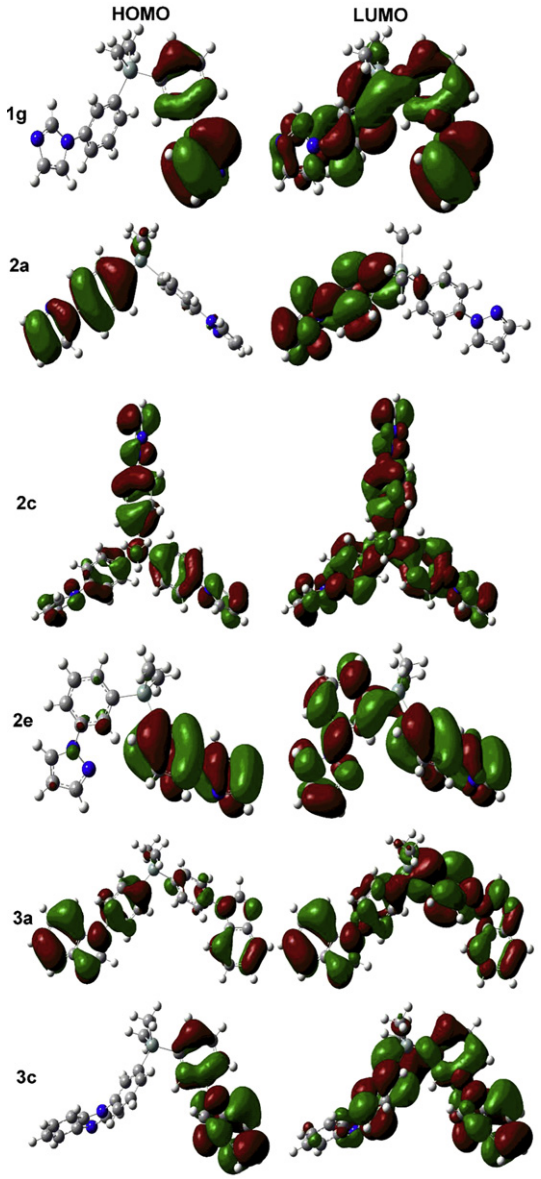

Fig. 4. Calculated spatial distributions of the HOMO and LUMO levels of compounds **1g**, **2a**, **2c**, **2e**, **3a** and **3c** as representatives.

reveal that the silanes with benzimidazole as functional groups and a *para*-disposition linkage are helpful to make the emission red-shift and higher thermal stability. It is beneficial to enhance the emission intensity through increasing the numbers of functional groups. The emission intensity of phenyl- or methyl-substituted compounds has almost no difference, which is also confirmed by molecular calculations. However, phenyl as substituent groups endowed compounds with higher thermal stability. These results may give valuable suggestions to select efficient luminescent materials for OLEDs. Further research will focus on the fabrication of efficient OLEDs based on these compounds as blue emitters, host materials or hole/electron blocking materials, as well as the construction of functional MOFs using these compounds as interesting tetrahedral building blocks and exploring their numerous potential applications in gas storage, catalysts, ion exchange, etc.

4. Experimental

4.1. General

Unless otherwise noted, all reagents were obtained from commercial suppliers and used without further purification. Dimethyl sulfoxide (DMSO) was firstly dried over CaH_2 at 80 °C for 1 day and distilled under vacuum pressure. Then DMSO was stored with 4 Å molecular sieves prior to use. Ether was dried by distillation from the sodium ketyl of benzophenone. FT-IR was recorded on a Bruker Tensor27 spectrophotometer in the frequency range 4000–400 cm^{-1} at a resolution of 4 cm^{-1} with a total of 32 scans. ^1H NMR and ^{13}C NMR spectra were measured on a Bruker AVANCE-300 or 400 NMR spectrometer. High-resolution mass spectra were obtained using positive mode on Agilent Technologies 6510 Q-TOF LC-MS. TGA was performed with a MettlerToledo SDTA-854 TGA system in nitrogen at a heating rate of 10 °C/min. DSC measurements were carried out in PerkinElmer DSC8500 series ramping from −10 to 250 °C at the rate of 10 °C/min under N_2. The fluorescence spectra were determined with F-7000 spectrophotometer. Luminescence quantum yields were measured using quinine sulfate in 0.1 N H_2SO_4 ($\Phi = 54.6\%$) as reference. The quantum yields were calculated according to the procedures described elsewhere [50,51].

4.2. Synthesis of (4-bromophenyl)silane (*4a*–*f*) and (3-bromophenyl)silane (*5a*–*c*)

(4-Bromophenyl)silane (**4a**–**f**) and (3-bromophenyl)silane (**5a**–**c**) were synthesized as our previous reports [44]. The typical synthetic procedure for the bromophenylsilanes is mentioned below.

1,4-Dibromobenzene or 1,3-dibromobenzene (1 equiv) was dissolved in dry Et_2O and cooled to −78 °C under argon. *n*-BuLi (1.05 equiv) was added into this solution dropwise and stirred for another 1 h at −78 °C. Chlorosilane (chlorotrimethylsilane: 1 equiv; dichlorodimethylsilane or dichlorodiphenylsilane: 0.5 equiv; trichloromethylsilane or trichlorophenylsilane: 0.33 equiv; tetrachlorosilane: 0.25 equiv) was then added dropwise at this temperature. After the end of the addition, the reaction mixture was slowly raised to room temperature and stirred overnight. Then the reaction was quenched by H_2O and the organic layer was separated. The water layer was washed twice by Et_2O. The organic layers were combined, washed by brine, dried over anhydrous $MgSO_4$ and then filtered. Removal of the solvents under vacuum gave the crude product and the pure products were obtained by column chromatography or recrystallization.

The physical and spectroscopic data of **4a**–**f** were shown in our previous report [44].

(3-Bromophenyl)trimethylsilane (**5a**) was afforded as a colorless liquid. Yield: 56.9%. IR (KBr pellet cm^{-1}): 3050, 2956, 2897, 1552, 1460, 1387, 1252, 1122, 1071, 1022, 993, 845, 749, 687. ^1H NMR (400 MHz, $CDCl_3$, ppm): 0.31 (s, 9H), 7.26 (t, $J = 7.6$ Hz, 1H), 7.46 (d, $J = 7.6$ Hz, 1H), 7.51 (d, $J = 7.6$ Hz, 1H), 7.66 (s, 1H).

Bis(3-bromophenyl)dimethylsilane (**5b**) was afforded as a colorless crystal. Yield: 77.8%. IR (KBr pellet cm^{-1}): 3047, 2958, 2871, 1551, 1464, 1384, 1254, 1124, 1085, 1068, 992, 821, 770, 687. ^1H NMR (300 MHz, $CDCl_3$, ppm): δ 0.58 (s, 6H), 7.25 (t, $J = 7.5$ Hz, 2H), 7.41 (d, $J = 7.5$ Hz, 2H), 7.53 (d, 2H, $J = 7.5$ Hz), 7.59 (s, 2H).

Tri(3-bromophenyl)methylsilane (**5c**) was afforded as a white solid. Yield: 60.5%. IR (KBr pellet cm^{-1}): 3074, 3006, 2962, 1568, 1549, 1476, 1376, 1252, 1110, 1066, 1009, 809, 781, 721. ^1H NMR (400 MHz, $CDCl_3$, ppm): 0.86 (s, 3H), 7.28 (t, $J = 7.9$ Hz, 3H), 7.39 (d, $J = 7.9$ Hz, 3H), 7.58 (d, $J = 7.9$ Hz, 3H), 7.60 (s, 3H).

4.3. Synthesis of imidazole functional silanes (*1a–i*)

Imidazole functionalized silanes were synthesized as our previous report [44]. The typical synthetic procedure is mentioned below.

Bromophenylsilane (1 equiv), imidazole (1.2 equiv calculated as molar percent of bromophenyl), K_2CO_3 (2 equiv calculated as molar percent of bromophenyl) and $CuSO_4$ (0.01 equiv calculated as molar percent of bromophenyl) were mixed and heated at 180 °C for 24 h in a Teflon autoclave under argon. After cooling to ambient temperature, the mixture was dissolved in CH_2Cl_2/H_2O (1:1) mixture. The water layer was separated and extracted with CH_2Cl_2 three times. The combined organic layers were washed with water, dried over anhydrous $MgSO_4$ and filtered. The solvents were evaporated under reduced pressure and the pure products were obtained by column chromatography (CH_2Cl_2/MeOH as eluent). The characterization of imidazole functional silanes, including bis(4-(imidazol-1-yl)phenyl)dimethylsilane (**1a**), tri(4-(imidazol-1-yl)phenyl)methylsilane (**1b**), bis(4-(imidazol-1-yl)phenyl)diphenylsilane (**1c**), tri(4-(imidazol-1-yl)phenyl)phenylsilane (**1d**) and [tri(4-(imidazol-1-yl)phenyl)] (4-bromophenyl)silane (**1e**) were shown in our previous report [44].

(3-(Imidazol-1-yl)phenyl)trimethylsilane (**1f**) was afforded as a yellow liquid. Yield: 65.3%. IR (KBr pellet cm^{-1}): 3105, 3029, 2953, 2860, 1596, 1511, 1443, 1392, 1291, 1249, 1228, 1109, 1061, 964, 816, 735, 660, 616, 534. ^1H NMR (400 MHz, DMSO) δ 8.28 (s, 1H), 7.76 (s, 1H), 7.69 (s, 1H), 7.59–7.62 (m, 1H), 7.48–7.49 (t, 2H), 0.28 (s, 9H). ^{13}C NMR (100 MHz, DMSO): δ 142.9, 135.8, 137.1, 135.8, 132.1, 130.3, 129.7, 125.4, 121.7, 120.8, −0.8. HRMS (FAB) calcd for $C_{12}H_{16}N_2Si$ (MH^+): 217.1156, found 217.1165. Anal. Calcd for $C_{12}H_{16}N_2Si$: C, 66.62; H, 7.45; N, 12.95. Found: C, 66.03; H, 7.38; N, 12.65.

Bis(3-(imidazol-1-yl)phenyl)dimethylsilane (**1g**) was afforded as a white solid. Yield: 45.5%. IR (KBr pellet cm^{-1}): 3117, 3035, 2952, 2856, 1582, 1494, 1413, 1300, 1247, 1115, 1053, 978, 904, 830, 791, 746, 695, 657, 449. ^1H NMR (400 MHz, DMSO) δ 8.25 (s, 2H), 7.76 (s, 2H), 7.74 (s, 2H), 7.60–7.66 (m, 2H), 7.52 (s, 2H), 7.49 (s, 2H), 7.12 (s, 2H), 0.66 (s, 6H). ^{13}C NMR (100 MHz, DMSO): δ 141.9, 137.1, 136.1, 132.9, 130.3, 129.9, 126.0, 122.1, 118.7, −2.5. HRMS (FAB) calcd for $C_{20}H_{20}N_4Si$ (MH^+): 345.1530, found 345.1533. Anal. Calcd for $C_{20}H_{20}N_4Si$: C, 69.73; H, 5.85; N, 16.26. Found: C, 69.66; H, 5.79; N, 16.33.

Tri(3-(imidazol-1-yl)phenyl)methylsilane (**1h**) was afforded as a white solid. Yield: 40.8%. IR (KBr pellet cm^{-1}): 3106, 3053, 2955, 1582, 1497, 1417, 1303, 1249, 1108, 1057, 979, 906, 791, 696, 657, 469. ^1H NMR (300 MHz, DMSO) δ 8.25 (s, 3H), 7.73–7.77 (m, 9H), 7.50–7.61 (m, 6H), 7.10 (s, 3H), 1.07 (s, 3H). ^{13}C NMR (75 MHz, DMSO): δ 139.4, 138.9, 137.9, 135.8, 132.1, 131.9, 128.6, 124.4, 120.4, −2.1. HRMS (FAB) calcd for $C_{28}H_{24}N_6Si$ (MH^+): 473.1904, found 473.1905. Anal. Calcd for $C_{28}H_{24}N_6Si$: C, 71.16; H, 5.12; N, 17.78. Found: C, 71.02; H, 5.12; N, 17.13.

4.4. Synthesis of pyrazole functional silanes (*2a–e*)

The synthesis procedures of pyrazole functional silanes (**2a–e**) were similar to those of **1a–h**.

Bis(4-(pyrazol-1-yl)phenyl)dimethylsilane (**2a**) was afforded as a white solid. Yield: 70.3%. IR (KBr pellet cm^{-1}): 3110, 3027, 2955, 2898, 1590, 1513, 1393, 1327, 1253, 1196, 1110, 1041, 932, 811, 763, 659, 519. ^1H NMR (300 MHz, DMSO) δ 8.52 (d, $J = 2.7$ Hz, 2H), 7.85 (d, $J = 8.4$ Hz, 4H), 7.75 (d, $J = 1.5$ Hz, 2H), 7.63 (d, $J = 8.4$ Hz, 4H), 6.55 (t, $J = 2.4$ Hz, 2H), 0.59 (s, 6H). ^{13}C NMR (75 MHz, DMSO): δ 142.1, 141.4, 136.3, 136.2, 128.7, 118.8, 108.9, −1.6. HRMS (FAB) calcd for $C_{20}H_{20}N_4Si$ (MH^+): 345.1530, found 345.1536. Anal. Calcd for $C_{20}H_{20}N_4Si$: C, 69.73; H, 5.85; N, 16.26. Found: C, 69.05; H, 5.53; N, 16.35.

Bis(4-(pyrazol-1-yl)phenyl)diphenylsilane (**2b**) was afforded as a light yellow solid. Yield: 62.5%. IR (KBr pellet cm^{-1}): 3030, 1592, 1514, 1392, 1326, 1254, 1189, 1104, 1035, 930, 825, 738, 698, 543. ^1H NMR (300 MHz, DMSO) δ 8.55 (d, $J = 2.7$ Hz, 2H), 7.95 (d, $J = 8.7$ Hz, 2H), 7.78 (d, $J = 1.5$ Hz, 2H), 7.61 (d, $J = 8.7$ Hz, 2H), 7.56–7.45 (m, 10H), 6.58 (t, $J = 2.1$ Hz, 2H). ^{13}C NMR (75 MHz, DMSO): δ 142.3, 141.9, 138.1, 136.8, 134.2, 131.8, 131.0, 129.3, 128.8, 119.0, 109.1. HRMS (FAB) calcd for $C_{30}H_{24}N_4Si$ (MH^+): 469.1843, found 469.1831. Anal. Calcd for $C_{30}H_{24}N_4Si$: C, 76.89; H, 5.16; N, 11.96. Found: C, 76.23; H, 5.17; N, 12.03.

Tri(4-(pyrazole-1-yl)phenyl)methylsilane (**2c**) was afforded as a white solid. Yield: 55.4%. IR (KBr pellet cm^{-1}): 3114, 3026, 2956, 1592, 1516, 1392, 1328, 1253, 1193, 1100, 1039, 930, 788, 745, 533. ^1H NMR (300 MHz, DMSO) δ 8.47 (d, $J = 2.4$ Hz, 3H), 7.84 (d, $J = 8.7$ Hz, 6H), 7.71 (d, $J = 1.8$ Hz, 3H), 7.56 (d, $J = 8.7$ Hz, 6H), 6.49–6.51 (m, 3H), 0.86 (s, 3H). ^{13}C NMR (75 MHz, DMSO): δ 142.2, 141.7, 137.1, 133.9, 128.8, 118.9, 109.0, −2.8. HRMS (FAB) calcd for $C_{28}H_{24}N_6Si$ (MH^+): 473.1904, found 473.1942. Anal. Calcd for $C_{20}H_{20}N_4Si$: Anal. Calcd for $C_{28}H_{24}N_6Si$: C, 71.16; H, 5.12; N, 17.78. Found: C, 71.02; H, 5.03; N, 17.85.

Tri(4-(pyrazole-1-yl)phenyl)phenylsilane (**2d**) was afforded as a light yellow solid. Yield: 50.4%. IR (KBr pellet cm^{-1}): 3132 , 3031, 1593, 1519, 1392, 1330, 1252, 1192, 1101, 1039, 931, 821, 740, 698, 554. ^1H NMR (300 MHz, DMSO) δ 8.56 (d, $J = 2.7$ Hz, 3H), 7.96 (d, $J = 8.7$ Hz, 6H), 7.79 (d, $J = 1.5$ Hz, 3H), 7.63 (d, $J = 8.4$ Hz, 6H), 7.54–7.45 (m, 6H), 6.58 (t, $J = 1.8$ Hz, 3H). ^{13}C NMR (75 MHz, DMSO): δ 142.3, 142.0, 141.9, 138.6, 138.1, 136.8, 136.4, 134.1, 131.7, 131.5, 131.1, 129.3, 128.8, 128.7, 120.2, 119.1, 109.1, 109.0. HRMS (FAB) calcd for $C_{33}H_{26}N_6Si$ (MH^+): 535.2061, found 535.2064. Anal. Calcd for $C_{33}H_{26}N_6Si$: C, 74.13; H, 4.90; N, 15.72. Found: C, 73.95; H, 4.91; N, 15.75.

Bis(3-(pyrazol-1-yl)phenyl)dimethylsilane (**2e**) was afforded as a viscous yellow solid. Yield: 70.3%. IR (KBr pellet cm^{-1}): 3130, 3028, 2960, 2898, 1592, 1516, 1392, 1327, 1248, 1097, 1044, 935, 817, 752, 655, 535. ^1H NMR (300 MHz, DMSO) δ 8.53 (d, $J = 2.4$ Hz, 2H), 8.00 (s, 2H), 7.83–7.87 (m, 2H), 7.73 (d, $J = 1.5$ Hz, 2H), 7.44–7.52 (m, 4H), 6.53 (t, $J = 2.1$ Hz, 2H), 0.64 (s, 6H). ^{13}C NMR (75 MHz, DMSO): δ 141.9, 140.4, 140.3, 132.7, 130.1, 128.8, 124.4, 120.4, 108.8, −1.9. HRMS (FAB) calcd for $C_{20}H_{20}N_4Si$ (MH^+): 345.1530, found 345.1522. Anal. Calcd for $C_{20}H_{20}N_4Si$: C, 69.73; H, 5.85; N, 16.26. Found: C, 69.66; H, 5.90; N, 16.29.

4.5. Synthesis of benzimidazole functional silanes (*3a–c*)

The synthesis procedures of benzimidazole functional silanes (**3a–c**) were similar to those of **1a–i**.

Bis(4-(benimidazol-1-yl)phenyl)dimethylsilane (**3a**) was afforded as a white solid. Yield: 55.1%. IR (KBr pellet cm^{-1}): 3050, 3022,

2955, 1592, 1505, 1451, 1372, 1320, 1288, 1255, 1228, 1105, 1066, 1006, 811, 739, 670, 577, 527. ^{1}H NMR (400 MHz, DMSO) δ 8.58 (s, 2H), 7.83 (d, J = 8.3 Hz, 4H), 7.77–7.79 (m, 2H), 7.73 (d, J = 8.3 Hz, 4H), 7.65–7.68 (m, 2H), 7.30–7.35 (m, 4H), 0.68 (s, 6H). ^{13}C NMR (100 MHz, DMSO): δ 144.4, 143.7, 137.6, 137.4, 136.1, 133.4, 124.0, 123.5, 123.0, 120.5, 111.2, −2.3. HRMS (FAB) calcd for $C_{28}H_{24}N_4Si$ (MH^+): 445.1843, found 445.1829. Anal. Calcd for $C_{28}H_{24}N_4Si$: C, 75.64; H, 5.44; N, 12.60. Found: C, 75.60; H, 5.35; N, 12.69.

Bis(4-(benimidazol-1-yl)phenyl)diphenylsilane (**3b**) was afforded as a gray solid. Yield: 45.1%. IR (KBr pellet cm^{-1}): 3056, 1594, 1501, 1453, 1376, 1290, 1232, 1194, 1109, 1011, 974, 829, 741, 701, 641, 582, 535. ^{1}H NMR (400 MHz, DMSO) δ 8.58 (s, 2H), 7.83 (d, J = 8.3 Hz, 4H), 7.77–7.80 (m, 6H), 7.72–7.74 (m, 2H), 7.60–7.63 (m, 4H), 7.50–7.55 (m, 6H), 7.32–7.35 (m, 4H). ^{13}C NMR (100 MHz, DMSO): δ 143.9, 143.1, 137.5, 137.4, 135.8, 134.4, 132.7, 132.6, 130.1, 128.3, 127.8, 123.5, 123.1, 122.5, 119.9, 110.1. HRMS (FAB) calcd for $C_{38}H_{28}N_4Si$ (MH^+): 569.2075, found 569.2082. Anal. Calcd for $C_{38}H_{28}N_4Si$: C, 80.25; H, 4.96; N, 9.85. Found: C, 80.20; H, 4.93; N, 9.89.

Bis(3-(benzimidazol-1-yl)phenyl)dimethylsilane (**3c**) was afforded as a light yellow solid. Yield: 50.7%. IR (KBr pellet cm^{-1}): 3055, 3032, 2955, 1591, 1493, 1451, 1399, 1289, 1254, 1228, 1199, 1108, 1043, 1002, 827, 787, 741, 694, 617, 538. ^{1}H NMR (400 MHz, DMSO, ppm) δ 8.58 (s, 2H), 7.83 (s, 2H), 7.77 (d, J = 8.3 Hz, 2H), 7.58–7.72 (m, 6H), 7.50 (d, J = 5.5 Hz, 2H), 7.23–7.31 (m, 4H), 0.70 (s, 6H). ^{13}C NMR (100 MHz, DMSO, ppm): δ 144.6, 142.8, 141.9, 138.2, 137.1, 136.1, 132.9, 130.3, 129.9, 126.0, 122.1, 118.7, 111.3, −2.6. HRMS (FAB) calcd for $C_{28}H_{24}N_4Si$ (MH^+): 445.1843, found 445.1856. Anal. Calcd for $C_{28}H_{24}N_4Si$: C, 75.64; H, 5.44; N, 12.60. Found: C, 75.61; H, 5.42; N, 12.65.

Acknowledgments

This research was supported by the National Natural Science Foundation of China (No. 21274080), Postdoctoral Science Foundation of China (No. 2012M511018), the Key Natural Science Foundation of Shandong Province of China (No. ZR2011BZ001) and Special Funds for Postdoctoral Innovative Projects of Shandong Province (No. 201103037).

Appendix A. Supplementary data

Supplementary data related to this article can be found at http://dx.doi.org/10.1016/j.jorganchem.2013.03.010.

References

[1] M.A. Baldo, D.F. O'Brien, Y. You, A. Shoustikov, S. Sibley, M.E. Thompson, S.R. Forrest, Nature 395 (1998) 151–154.
[2] U. Mitschke, P. Baüerle, J. Mater. Chem. 10 (2000) 1471–1507.
[3] T.W. Kelley, P.F. Baude, C. Gerlach, D.E. Ender, D. Muyres, M.A. Haase, D.E. Vogel, S.D. Theiss, Chem. Mater. 16 (2004) 4413–4422.
[4] D. Dini, Chem. Mater. 17 (2005) 1933–1940.
[5] Y. Shirota, H. Kageyama, Chem. Rev. 107 (2007) 953–1010.
[6] A. Köhnen, K. Meerholz, M. Hagemann, M. Brinkmann, S. Sinzinger, Appl. Phys. Lett. 92 (2008) 3305–3309.
[7] H. Wu, L. Ying, W. Yang, Y. Cao, Chem. Soc. Rev. 38 (2009) 3391–3400.
[8] C.A. Zuniga, S. Barlow, S.R. Marder, Chem. Mater. 23 (2011) 658–681.
[9] L. Xiao, Z. Chen, B. Qu, J. Luo, S. Kong, Q. Gong, J. Kido, Adv. Mater. 23 (2011) 926–952.
[10] A. Chaskar, H.-F. Chen, K.-T. Wong, Adv. Mater. 23 (2011) 3876–3895.
[11] S. Reineke, F. Lindner, G. Schwartz, N. Seidler, K. Walzer, B. Lüssem, K. Leo, Nature 459 (2009) 234–238.
[12] S.A. Ponomarenko, S. Kirchmeyer, Adv. Polym. Sci. 235 (2011) 33–110.
[13] S. Gong, Y. Zhao, C. Yang, C. Zhong, J. Qin, D. Ma, J. Phys. Chem. C 114 (2010) 5193–5198.
[14] S. Gong, Y. Zhao, M. Wang, C. Yang, C. Zhong, J. Qin, D. Ma, Chem. Asian J. 5 (2010) 2093–2099.
[15] Z. Jiang, Z. Liu, C. Yang, C. Zhong, J. Qin, G. Yu, D. Ma, Adv. Funct. Mater. 19 (2009) 3987–3995.
[16] L. Chen, C. Yang, J. Qin, J. Gao, D. Ma, Inorg. Chim. Acta 359 (2006) 4207–4214.
[17] X.M. Liu, J. Xu, X. Lu, C. He, Org. Lett. 7 (2005) 2829–2832.
[18] Q. Shen, S.Y. Ye, G. Yu, P. Lu, Y.Q. Liu, Synth. Met. 158 (2008) 1054–1058.
[19] X. Ren, J. Li, R.J. Holmes, P.I. Djurovich, S.R. Forrest, M.E. Thompson, Chem. Mater. 16 (2004) 4743–4747.
[20] S.H. Kim, J. Jang, S.J. Lee, J.Y. Lee, Thin Solid Films 517 (2008) 722–726.
[21] S. Gong, Y. Chen, J. Luo, C. Yang, C. Zhong, J. Qin, D. Ma, Adv. Funct. Mater. 21 (2011) 1168–1178.
[22] S. Gong, Y. Chen, X. Zhang, P. Cai, C. Zhong, D. Ma, J. Qin, C. Yang, J. Mater. Chem. 21 (2011) 11197–11204.
[23] X.M. Liu, C. He, J. Huang, J. Xu, Chem. Mater. 17 (2005) 434–441.
[24] W. Nakanishi, S. Hitosugi, A. Piskareva, Y. Shimada, H. Taka, H. Kita, H. Isobe, Angew. Chem. Int. Ed. 49 (2010) 7239–7242.
[25] K.H. Lee, L.K. Kang, J.Y. Lee, S. Kang, S.O. Jeon, K.S. Yook, J.Y. Lee, S.S. Yoon, Adv. Funct. Mater. 20 (2010) 1345–1358.
[26] S. Gong, Q. Fu, Q. Wang, C. Yang, C. Zhong, J. Qin, D. Ma, Adv. Mater. 23 (2011) 4956–4959.
[27] S. Gong, Y. Chen, C. Yang, C. Zhong, J. Qin, D. Ma, Adv. Mater. 22 (2010) 5370–5373.
[28] S. Gong, C. Zhong, Q. Fu, D. Ma, J. Qin, C. Yang, J. Phys. Chem. C 117 (2013) 549–555.
[29] L.-H. Chan, R.-H. Lee, C.-F. Hsieh, H.-C. Yeh, C.-T. Chen, J. Am. Chem. Soc. 124 (2002) 6469–6479.
[30] Y.-Y. Lyu, J. Kwak, O. Kwon, S.-H. Lee, D. Kim, C. Lee, K. Char, Adv. Mater. 20 (2008) 2720–2729.
[31] M.-F. Wu, S.-J. Yeh, C.-T. Chen, H. Murayama, T. Tsuboi, W.-S. Li, I. Chao, S.-W. Liu, J.-K. Wang, Adv. Funct. Mater. 17 (2007) 1887–1895.
[32] D.-R. Bai, X.-Y. Liu, S.N. Wang, Chem. Eur. J. 13 (2007) 5713–5723.
[33] T. Lee, K.H. Song, I. Jung, Y. Kang, S.-H. Lee, S.O. Kang, J. Ko, J. Organomet. Chem. 691 (2006) 1887–1896.
[34] Y. You, C.-G. An, J.-J. Kim, S.Y. Park, J. Org. Chem. 72 (2007) 6241–6246.
[35] K.H. So, R. Kim, H. Park, I. Kang, K. Thangaraju, Y.S. Park, J.J. Kimc, S.-K. Kwon, Y.-H. Kim, Dyes Pigm. 92 (2011) 603–609.
[36] S.-O. Kim, Q. Zhao, K. Thangaraju, J.J. Kim, Y.-H. Kim, S.-K. Kwon, Dyes Pigm. 90 (2011) 139–145.
[37] G. Huang, C. Yang, Z.T. Xu, H.H. Wu, J. Li, M. Zeller, A.D. Hunter, S.S.-Y. Chui, C.-M. Che, Chem. Mater. 21 (2009) 541–546.
[38] S.E. Wenzel, M. Fischer, F. Hoffmann, M. Fröba, Inorg. Chem. 48 (2009) 6559–6565.
[39] M.M. Maye, J. Luo, I.I.S. Lim, L. Han, N.N. Kariuki, D. Rabinovich, T.B. Liu, C.J. Zhong, J. Am. Chem. Soc. 127 (2005) 1519–1529.
[40] B.I. Park, I. Sung Chun, Y.-A. Lee, K.-M. Park, O.-S. Jung, Inorg. Chem. 45 (2006) 4310–4313.
[41] R.P. Davies, R. Less, P.D. Lickiss, K. Robertson, A.J.P. White, Cryst. Growth Des. 10 (2010) 4571–4581.
[42] W.-S. Han, H.-J. Son, K.-R. Wee, K.-T. Min, S. Kwon, I.-H. Suh, S.-H. Choi, D.H. Jung, S.O. Kang, J. Phys. Chem. C 113 (2009) 19686–19693.
[43] D. Hu, P. Lu, C. Wang, H. Liu, H. Wang, Z. Wang, T. Fei, X. Gu, Y. Ma, J. Mater. Chem. 19 (2009) 6143–6148.
[44] D.X. Wang, Y.Z. Niu, Y.K. Wang, J.J. Han, S.Y. Feng, J. Organomet. Chem. 695 (2010) 2329–2337.
[45] Q.Y. Ma, D.X. Wang, J. Inorg. Organomet. Poly 21 (2011) 797–801.
[46] D.X. Wang, H.Y. He, X.H. Chen, S.Y. Feng, Y.Z. Niu, D.F. Sun, CrystEngCommun 12 (2010) 1041–1043.
[47] D.X. Wang, Synthesis, Assembly and Properties of N-heterocycle and Carboxylate Functionalized Silanes, Shandong University Doctoral Dissertation, 2011.
[48] P.I. Shih, C.-H. Chien, C.-Y. Chuang, C.-F. Shu, C.-H. Yang, J.-H. Chen, Y. Chi, J. Mater. Chem. 17 (2007) 1692–1698.
[49] M.J. Frisch, G.W. Trucks, H.B. Schlegel, G.E. Scuseria, M.A. Robb, J.R. Cheeseman, J.A. Montgomery Jr., T. Vreven, K.N. Kudin, J.C. Burant, J.M. Millam, S.S. Iyengar, J. Tomasi, V. Barone, B. Mennucci, M. Cossi, G. Scalmani, N. Rega, G.A. Petersson, H. Nakatsuji, M. Hada, M. Ehara, K. Toyota, R. Fukuda, J. Hasegawa, M. Ishida, T. Nakajima, Y. Honda, O. Kitao, H. Nakai, M. Klene, X. Li, J.E. Knox, H.P. Hratchian, J.B. Cross, C. Adamo, J. Jaramillo, R. Gomperts, R.E. Stratmann, O. Yazyev, A.J. Austin, R. Cammi, C. Pomelli, J.W. Ochterski, P.Y. Ayala, K. Morokuma, G.A. Voth, P. Salvador, J.J. Dannenberg, V.G. Zakrzewski, S. Dapprich, A.D. Daniels, M.C. Strain, O. Farkas, D.K. Malick, A.D. Rabuck, K. Raghavachari, J.B. Foresman, J.V. Ortiz, Q. Cui, A.G. Baboul, S. Clifford, J. Cioslowski, B.B. Stefanov, G. Liu, A. Liashenko, P. Piskorz, I. Komaromi, R.L. Martin, D.J. Fox, T. Keith, M.A. Al-Laham, C.Y. Peng, A. Nanayakkara, M. Challacombe, P.M.W. Gill, B. Johnson, W. Chen, M.W. Wong, C. Gonzalez, J.A. Pople, Gaussian 03, Revision B.04, Gaussian, Inc., Pittsburgh, PA, 2003.
[50] S.R. Meech, D.C. Philips, J. Photochem. 65 (1983) 229.
[51] J.P. Cross, M. Lauz, P.D. Badger, S. Petoud, J. Am. Chem. Soc. 126 (2004) 16278.